The Dynemicin-DNA Intercalation Complex. A Model Based on DNA Affinity Cleavage and Molecular Dynamics Simulation

D. R. Langley,*,†,‡ T. W. Doyle,† and D. L. Beveridge‡

Contribution from the Chemistry Department, Hall-Atwater Laboratories, Wesleyan University, Middletown, Connecticut 06457, and Bristol-Myers Squibb Company, Pharmaceutical Research Institute, 5 Research Parkway, P.O. Box 5100, Wallingford, Connecticut 06492-7660.
Received June 15, 1990

Abstract: A model for the dynemicin-DNA complex has been constructed by using energy minimization (EM) and molecular dynamics (MD) techniques. The model is consistent with the available experimental data. This has allowed us to gain insights into (1) how dynemicin A is activated into a DNA cleaver, (2) its mode of binding to DNA, (3) the absolute stereochemistry of dynemicin A, and (4) its DNA cleavage patterns and specificity.

Dynemicin A (BMY-28646, BU-3420T) (Figure 1) is a violet-colored metabolite, of *Micromonospora chersina* sp. nov. N956-1 isolated from a soil sample found in Gujarat state, India,[1] with potent activity against a wide range of bacteria and various tumor cell lines.

The novel structure and relative stereochemistry of dynemicin A has been determined through spectroscopic and X-ray diffraction studies.[1b] The heptacyclo-1,5-diyn-3-ene ring system is a hybrid of an anthraquinone (DNA intercalater[2]) and a 1,5-diyn-3-ene (diradical generator[3]). Dynemicin A is the newest member of the enediyne containing class of compounds, which includes neocarzinostatin,[4] the esperamicins,[5] and calicheamicins.[6]

The mechanism of action by which dynemicin A exerts its biological activity is believed to be due to its ability to cause DNA strand breaks.[7] Presumably, the anthraquinone core of dynemicin intercalates into the DNA positioning the enediyne ring so that efficient DNA hydrogen abstraction occurs when it fires to the aryl diradical. To test the validity of this assumption we decided to use energy minimization (EM) and molecular dynamics (MD) modeling techniques to build a model of the dynemicin-DNA complex.

Drug Activation

The opening of the epoxide in dynemicin A is believed to be the key step in the activation to the aryl diradical[8] (DNA cleaving intermediate). The epoxide, like the bridge head double bond in esperamicin A,[3a] locks the conformation of the 1,5-diyn-3-ene system so that C23 and C28 are too far apart for bonding interaction,[9] 3.53 Å apart in dynemicin A and 3.34 Å apart in esperamicin A_1, based on the CHARMM[10] force field. The opening of the epoxide in dynemicin, or the elimination of the bridge head double bond in esperamicin A_1, relieves the ring strain and allows the ends of the enediyne system to move closer together (3.14 and 3.19 Å apart for dynemicin diol and alcohol forms, respectively, and 3.17 Å for esperamicin A_1). This in turn reduces the strain energy required in the diradical transition state[8b,9b-d] and allows for the formation of the aryl diradicals via a Bergman[11] type reaction at ambient temperatures. The diradical intermediate can now abstract hydrogens from either the solvent or the DNA giving an aromatized form of dynemicin or esperamicin Z.

Epoxides can be opened under both basic and acidic conditions to give diols or halohydrins. However at physiological pH, epoxides are relatively stable. By using the work of Koch[12] and Fisher[13] as a precedent, a reasonable mechanism for the epoxide ring-opening reaction would require the conversion of dynemicin A (**1**, Scheme I) to the hydroquinone **2** via a two-electron or two-sequential one-electron reduction(s) followed by an epoxide ring-opening reaction producing the quinonemethide **3**. The quinonemethide can now undergo nucleophilic attack by water or be protonated giving the diol **4** or the alcohol **5**, respectively. Compounds **4** and **5** can now undergo the Bergman reaction and aromatize, via diradical intermediates, affording dynemicin N

† Bristol-Myers Squibb Company.
‡ Wesleyan University.

(1) (a) Konishi, M.; Ohkuma, H.; Matsumoto, K.; Tsuno, T.; Kamei, H.; Miyaki, T.; Oki, T.; Kawaguchi, H.; VanDuyne, G. D.; Clardy, J. *J. Antibiot.* **1989**, *42*, 1449. (b) Konishi, M.; Ohkuma, H.; Tsuno, T.; Oki, T.; VanDuyne, G. D.; Clardy, J. *J. Am. Chem. Soc.* **1990**, *112*, 3715.

(2) (a) Quigley, G. J.; Wang, A. H.-J.; Ughetto, G.; Marel, G.; VanBoom, J.; Rich, A. *Proc. Natl. Acad. Sci. U.S.A.* **1980**, *77*, 12, 7204. (b) Wang, A. H.-J.; Ughetto, G.; Quigley, G. J.; Rich, A. *Biochemistry* **1987**, *26*, 1152. (c) Moore, M. H.; Hunter, W. N.; d'Estaintot, B. L.; Kennard, O. J. *Mol. Biol.* **1989**, *206*, 693. (d) Frederick, C. A.; Williams, L. D.; Ughetto, G. van der Marel, G. A.; van Boom, J. H.; Rich, A.; Wang, A. H.-J. *Biochemistry* **1990**, *29*, 2538.

(3) (a) Long, B. H.; Golik, J.; Forenza, S.; Ward, B.; Rehfuss, R.; Dabrowiak, J. C.; Catino, J. J.; Musial, S. T.; Brookshire, K. W.; Doyle, T. W. *Proc. Natl. Acad. Sci. U.S.A.* **1989**, *86*, 2. (b) Sugiura, Y.; Uesawa, Y.; Takahashi, Y.; Kuwahara, J.; Golik, J.; Doyle, T. W. *Proc. Natl. Acad. Sci. U.S.A.* **1989**, *86*, 7672. (c) Kozarich, J. W.; Worth, L., Jr.; Frank, B. L.; Christner, D. F.; Vanderwall, D. E.; Stubbe, J. *Science* **1989**, *245*, 1396. (d) Zein, N.; Sinha, A. M.; McGahren, W. J.; Ellestad, G. A. *Science* **1988**, *240*, 1198. (e) Zein, N.; Poncin, M.; Nilakatan, R.; Ellestad, G. A. *Science* **1989**, *244*, 697.

(4) (a) Edo, K.; Mizugaki, M.; Koide, Y.; Seto, H.; Furihata, K.; Otake, N.; Ishida, N. *Tetrahedron Lett.* **1985**, *26*, 331. (b) Myers, A. G.; Proteau, P. J.; Handel, T. M. *J. Am. Chem. Soc.* **1988**, *110*, 7212. (c) Galat, A.; Goldberg, I. H. *Nucleic Acid Res.* **1990**, *18*, 2093.

(5) (a) Golik, J.; Clardy, J.; Dubay, G.; Groenewold, G.; Kawaguchi, H.; Konishi, M.; Krishnan, B.; Ohkuma, H.; Saitoh, K. I.; Doyle, T. W. *J. Am. Chem. Soc.* **1987**, *109*, 3461. (b) Golik, J.; Dubay, G.; Groenewold, G.; Kawaguchi, H.; Konishi, M.; Krishnan, B.; Ohkuma, H.; Saitoh, K. I.; Doyle, T. W. *J. Am. Chem. Soc.* **1987**, *109*, 3462.

(6) (a) Lee, M. D.; Dunne, T. S.; Siegel, M. M.; Chang, C. C.; Morton, G. O.; Borders, D. B. *J. Am. Chem. Soc.* **1987**, *109*, 3464. (b) Lee, M. D.; Dunne, T. S.; Chang, C. C.; Ellestad, G. A.; Siegel, M. M.; Morton, G. O.; McGahren, W. J.; Borders, D. B. *J. Am. Chem. Soc.* **1987**, *109*, 3466.

(7) Sugiura, Y.; Shiraki, T.; Konishi, M.; Oki, T. *Proc. Nat. Acad. Sci. U.S.A.* **1990**, *87*, 3831.

(8) (a) Semmelhack, M. F.; Gallagher, J.; Cohen, D. *Tetrahedron Lett.* **1990**, *31*, 1521. (b) Snyder, J. P.; Tipsword, G. E. *J. Am. Chem. Soc.* **1990**, *112*, 4040. (d) Stinson, S. *Chem. Eng. News* **1990**, May 28, 22.

(9) (a) Nicolaou, K. C.; Zuccarello, G.; Ogawa, Y.; Schweiger, E. J.; Kumazawa, T. *J. Am. Chem. Soc.* **1988**, *110*, 4866. (b) Snyder, J. P. *J. Am. Chem. Soc.* **1989**, *111*, 7630. (c) Magnus, P.; Fortt, S.; Pitterna, T.; Snyder, J. P. *J. Am. Chem. Soc.* **1990**, *112*, 4986. (d) Snyder, J. P. *J. Am. Chem. Soc.* **1990**, *112*, 5367.

(10) Brooks, B. R.; Bruccoleri, R. E.; Olafson, B. D.; States, D. J.; Swaminathan, S.; Karplus, M. *J. Comput. Chem.* **1983**, *4*, 187.

(11) (a) Lockhart, T. P.; Comits, P. B.; Bergman, R. G. *J. Am. Chem. Soc.* **1981**, *103*, 4082. (b) Bergman, R. G. *Acc. Chem. Res.* **1973**, *6*, 25.

(12) (a) Boldt, M.; Gaudiano, G.; Haddadin, M. J.; Koch, T. H. *J. Am. Chem. Soc.* **1989**, *111*, 2283. (b) Kleyer, D. L.; Koch, T. H. *J. Am. Chem. Soc.* **1984**, *106*, 2380. (c) Boldt, M.; Guadiano, G.; Koch, T. H. *J. Am. Chem. Soc.* **1987**, *52*, 2146. (d) Boldt, M.; Gaudiano, G.; Haddadin, M. J.; Koch, T. H. *J. Am. Chem. Soc.* **1988**, *110*, 3330.

(13) Fisher, J.; Abdella, B. R. J.; McLane, K. E. *Biochemistry* **1985**, *24*, 3562.

0002-7863/91/1513-4395$02.50/0

Scheme I

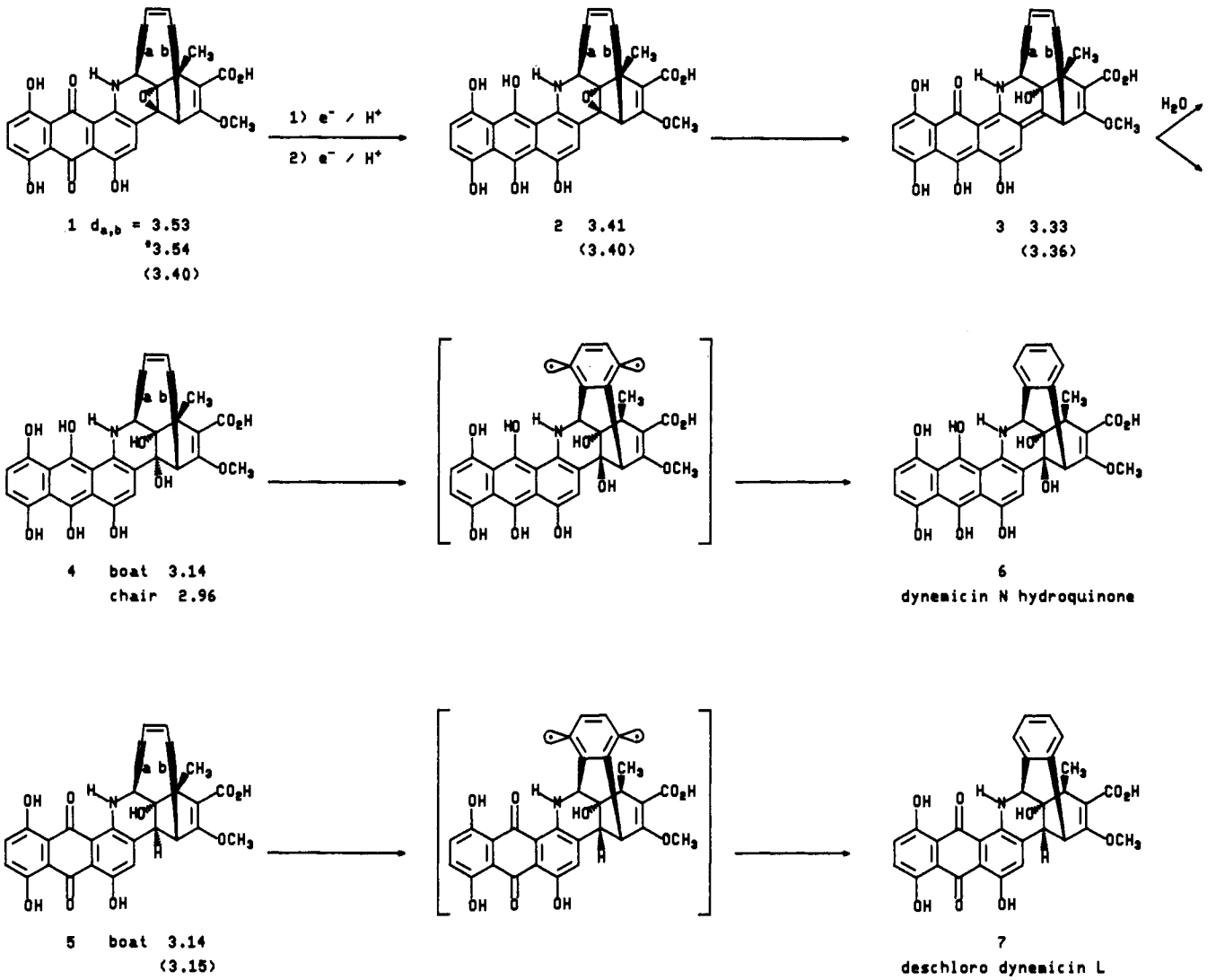

hydroquinone (**6**) and deschlorodynemicin L (dynemicin H)[14] (**7**).

Snyder and Tipsword[8b] recently proposed a similar mechanism of activation for dynemicin A by analogy with the anthracycline menogaril and compared the relative ease of converting dynemicin A and menogaril to their respective quinonemethides by using MM2//PRDDO. They found that the reduction of the dynemicin A (**1**, Scheme I) quinone to the hydroquinone **2** is favored over the same process for menogaril by 3.9 kcal. The opening of the epoxide or elimination of methoxide for dynemicin hydroquinone (**2**) and menogaril hydroquinone giving dynemicin **3** and menogaril quinonemethides, respectively, was found to be favored for the dynemicin system by 45.2 kcal. The rearrangement of the dynemicin quinonemethide **3** to the alcohol **4** was PRDDO predicted to be exothermic by 22.8 kcal. The alcohol was then predicted to aromatize via an energy barrier of $\Delta E^* = 19.2$ kcal to the biradical transition state. Alternatively, addition of methoxide to the quinonemethide **3** was predicted to reduces the strain energy in the transition state allowing aromatization of the resulting hydroquinone via an energy barrier of $\Delta E^* = 19.1$ kcal.

Dynemicin Sequence Specific Cleavage of DNA

Sugiura's group[7] has conducted DNA cleavage experiments with dynemicin. In this study it was shown that dynemicin can be reductively activated to yield a DNA cleaver that causes the conversion of form I DNA into forms II and III DNA and that the rate of conversion is dependent on the type of reducing agent. In their affinity cleavage experiments they demonstrated that NADPH reduction of dynemicin produced site-specific cleavage of DNA (Figure 2) and that these sites could be predictively inhibited by sequence-specific minor groove binders, alkylators, and intercalators. Furthermore it was reported that dynemicin preferentially cuts the DNA at the base immediately to the 3′-side of purines, and these cut 5′-^{32}P-labeled oligomers produced radioactive bands that were electrophoretically identical with the Maxam and Gilbert products,[15] indicating that the drug abstracts a 5′- and/or 5″-hydrogen from the DNA backbone.[16]

Reevaluation of Cleavage Affinity Data

A preliminary model of the dynemicin–DNA intercalation complex suggested that dynemicin intercalates between the two bases immediately to the 5′-side of the cut site. To verify this we reanalyzed the histogram and relative intensity of DNA cut sites produced by the dynemicin–NADPH system.[7] The cuts were categorized into 5′-B2-B1-Ct domains where B1 and B2 are purine (Pu) or pyrimidine (Py) bases and Ct is the cut site. The domains were then divided into strong, medium, and weak cuts based on their height relative to the strongest cut site (Table I), as determined by densitometric scanning.

(14) Dabrah, T. T.; Matson, J. A., personal communication. Deschlorodynemicin L has been isolated from the *Micromonospora chersina* sp. nov. N956-1 fermentation broth along with dynemicin A and dynemicin N. Deschlorodynemicin L (dynemicin H) was found to be the major product formed when dynemicin A was activated with visible light. Shiraki, T.; Sugiura, Y. *Biochemistry* **1990**, *29*, 9795.

(15) Maxam, A.; Gilbert, W. *Methods Enzymol.* **1990**, *65*, 499.

(16) Kappen, L. S.; Goldberg, I. H. *Biochemistry* **1983**, *22*, 4872.

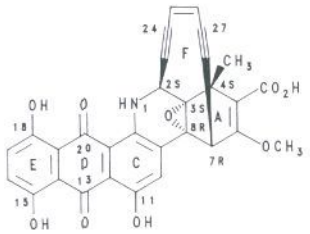

Figure 1. Dynemicin A (BMY-28646).

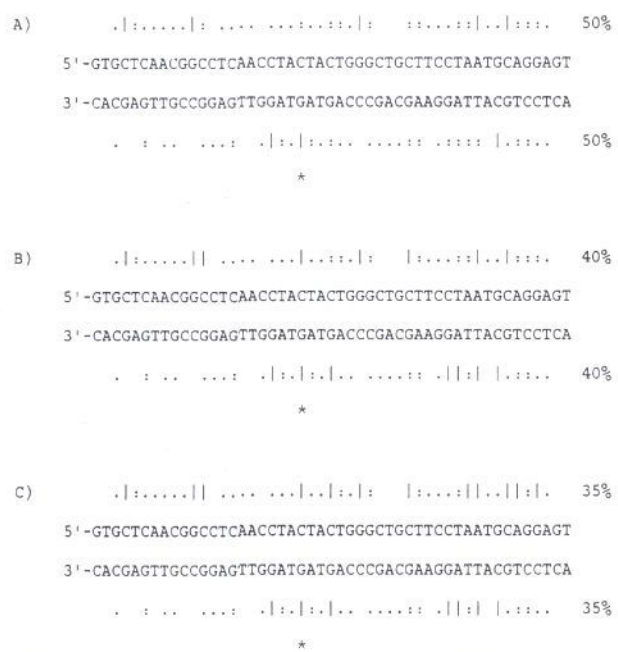

Figure 2. Histogram of cleavage sites on the 5′-^{32}P-labeled (SalI-DraII) pBR322 DNA restriction fragment produced by NADPH/dynemicin A, strongest (*), strong (|), medium (:), and weak (·) cleavage sites and strong ≥ X > medium ≥ 20% > weak cuts: (A) X = 50% of the strongest cut site, (B) X = 40%, and (C) X = 35%.

The cutoffs used in assigning strong, medium, and weak sites were arbitrarily chosen. Intensities equal to or greater than 50%, 40%, and 35% of the strongest cut site (*) were assigned to strong cut sites in panels A, B, and C of Figure 2, respectively. All sites with intensities less than 20% of the strongest cut site were assigned to weak or background cuts. The analysis leads to the same conclusions regardless of which criteria for selection is used in determining strong sites. However, the 20% and 40% cutoffs best divide the cut sites into natural groups and was used in the analysis reported in Table I.

At low concentrations of drug the highest affinity cleavage sites will be produced first. If the drug concentration is sufficiently high, then secondary, and finally tertiary, sites will produce cuts. With a drug as potent as dynemicin, the intercellular drug concentration can be assumed to be very low; therefore, only the highest affinity sites are expected to produce the cuts that lead to the biological response. It is for this reason that only the strong cleavage sites were used to determine the sequence specificity for dynemicin.

The preferred cutting site for dynemicin is 5′-Py-Pu-Ct (Table I). The order of sequence specificity is Py-Pu-Ct ≫ Py-Py-Ct = Pu-Pu-Ct = Pu-Py-Ct. When the sequences were broken down into their respective bases, a preference of TACt = TGCt > CGCt > CACt > TTCt > GGCt was found. Analyzing the 5′-B3-Py-Pu-Ct domains for B3 or Ct base preference (Table II) revealed a slight preference for a G or C in the Ct site over an A or T and suggests that the drug prefers not to have a T in the B3 site.

Goals and Limitations

It is the goal of this work to develop a dynemicin–DNA model that is consistent with the available experimental data. The model will then be used to gain insights into the mechanism of activation of dynemicin A, its mode of binding to DNA, the absolute stereochemistry of dynemicin A, and its DNA pattern and sequence specificity of cleavage.

It is important to keep in mind that solvent (water) and counterions are not included in the model. As a result, hydrogen bonds that occur in a solvent accessible region will be overstated. Likewise, structural water molecules are missing which are ex-

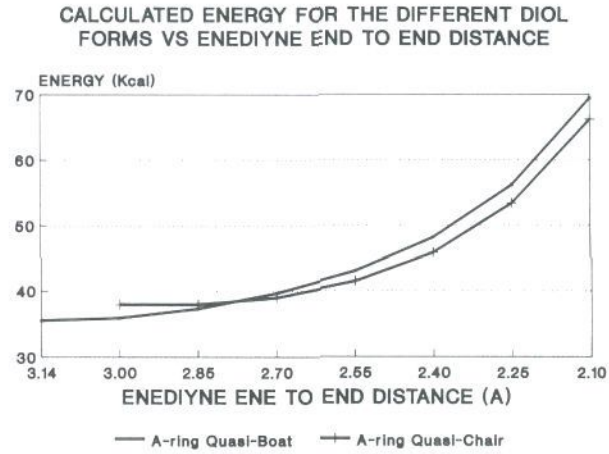

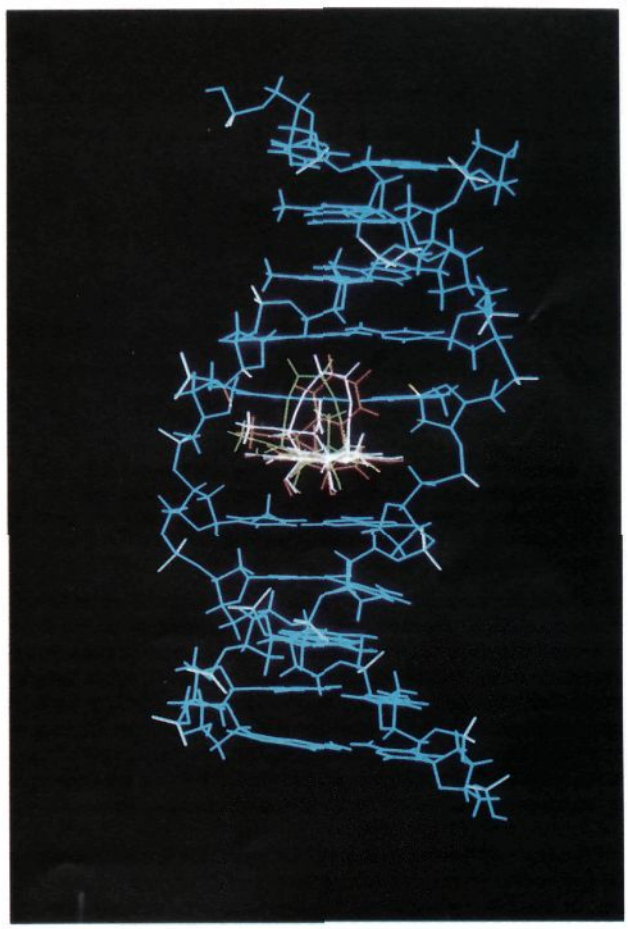

Figure 3. (a, top) Energy for the diol **4** quasi-boat (−) and quasi-chair (+) forms vs enediyne end-to-end distance. (b, bottom) The superimposed EM form of the diol **4** quasi-boat (green), quasi-chair (purple), and dynemicin N hydroquinone (**6**) (red) intercalated into the d-(CTACT_ACTGG)·d(CCAGT_AGTAG) duplex DNA. The coloring scheme for the DNA is blue and light blue for the free phosphate oxygens. The red and white hydrogens of guanine 17 are H5′ and H1′, and the yellow and green hydrogens of thymine 5 are H1′ and H2′, respectively.

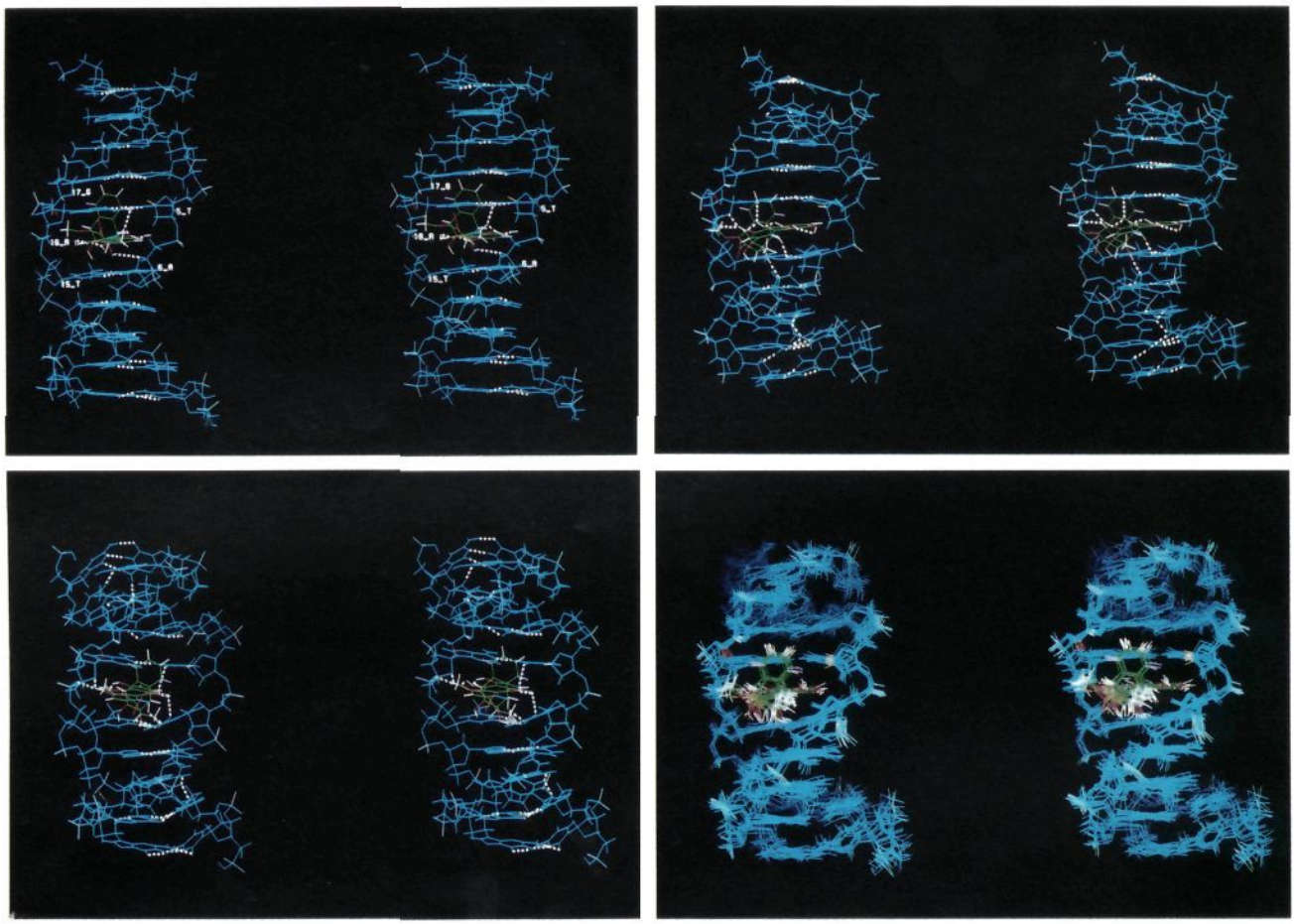

Figure 4. Stereoviews of (a, top left) the EM complex between (2*S*,7*R*)-dynemicin N hydroquinone and the d(CTACT_ACTGG)·(CCAGT_AGTAG) duplex oligonucleotide. (b, top right) Snapshot of the 19-ps frame from the dynamics animation. (c, bottom left) Snapshot of the 55-ps snapshot frame. (d, bottom right) Composite of seven snapshots taken every 5 ps from 80 ps to the end of the dynamics animation. The coloring scheme for the DNA is the same as in Figure 3b; the drug colors are carbon (green), nitrogen (blue), oxygen (red), hydrogen (white), and C27–H (left) and C24–H (right) bonds are violet. The white dotted lines represent hydrogen bonds.

Table I. Statistical Analysis of Histogram Panel B (Figure 2)

5′-B2-B1-Ct domain	possible binding sites	strong cuts (%)	medium cuts (%)	weak cuts (%)
Pu-Pu-Ct	23	1 (4.3)	4 (17.4)	12 (52.2)
Pu-Py-Ct	21		7 (33.3)	7 (33.3)
Py-Pu-Ct	21	13 (61.9)	2 (10.0)	5 (23.8)
Py-Py-Ct	25	1 (4.0)	6 (24.0)	17 (68.0)
A-A-Ct	4		1 (25.0)	2 (50.0)
A-G-Ct	9		1 (11.1)	8 (88.9)
G-A-Ct	3		1 (33.3)	1 (66.7)
G-G-Ct	7	1 (14.3)	1 (14.3)	1 (14.3)
A-T-Ct	2		1 (50.0)	1 (50.0)
A-C-Ct	5		1 (20.0)	5 (80.0)
G-T-Ct	5		2 (40.0)	1 (20.0)
G-C-Ct	9		3 (33.3)	1 (11.1)
T-A-Ct	6	5 (83.3)	1 (16.7)	
T-G-Ct	7	5 (71.4)		1 (14.3)
C-A-Ct	6	2 (33.3)	1 (16.7)	3 (50.0)
C-G-Ct	2	1 (50.0)		1 (50.0)
T-T-Ct	4	1 (25.0)	2 (50.0)	1 (25.0)
T-C-Ct	4		1 (25.0)	3 (75.0)
C-C-Ct	7		2 (28.6)	5 (71.4)
C-T-Ct	10		1 (10.0)	8 (80.0)

pected to effect the micro structure of the DNA and its complexes.[2,17] The calculations rely on an assumed force field and our chemical intuition to correctly use the force field. Due to these limitations it is important to have good experimental data which can be used as a guide in model building and as a reference to verify that the calculations are proceeding in the right direction.

Criteria Used To Validate the Model

From the cleavage affinity experiments[7] we know that at least part of the dynemicin molecule binds in the minor groove of the DNA, that it has a sequence specifity of 5′-Py-Pu-Ct, that either the 5′- and/or 5″-hydrogen of the Ct base is abstracted, and that the major cut site is at the guanine (*, Figure 2) in the 5′-TAG sequence. From the MM2//PRDDO studies[9b] we know that the geometry of the diradical transition state is much more benzene-like, i.e., the bond angles for the acetylene atoms are much closer to 120° than 180°. On the basis of the above experimental and theoretical observations, the following criteria will be used in model building and validation of the model. A model between either dynemicin N hydroquinone (**6**) or deschlorodynemicin L (**7**) and DNA should place at least a portion of the drug in the minor groove and interacting with the 5′-Py-Pu bases of a 5′-Py-Pu-Ct sequence. The docked complex should also place C24 and/or C27 of the drug near either a DNA H5′- or H5″-hydrogen.

The C–C–H bond angle for benzene is 120°. Assuming that the 1,4-diradical has a similar geometry as a benzene hydrogen, a DNA hydrogen that lies along the benzene C–H vector would be aligned with the radical orbital. Given two hydrogens of equal distance from the radical-centered carbon, the one aligned most closely with the axis of the radical orbital will be abstracted.[18]

(17) (a) Drew, H. R.; Dickerson, R. E. *J. Mol. Biol.* **1981**, *151*, 535. (b) Kopka, M. L.; Fratini, A. V.; Drew, H. R.; Dickerson, R. E. *J. Mol. Biol.* **1983**, *163*, 129.

(18) Hawley, R. C.; Kiessling, L. L.; Schreiber, S. L. *Proc. Natl. Acad. Sci. U.S.A.* **1989**, *86*, 1105.

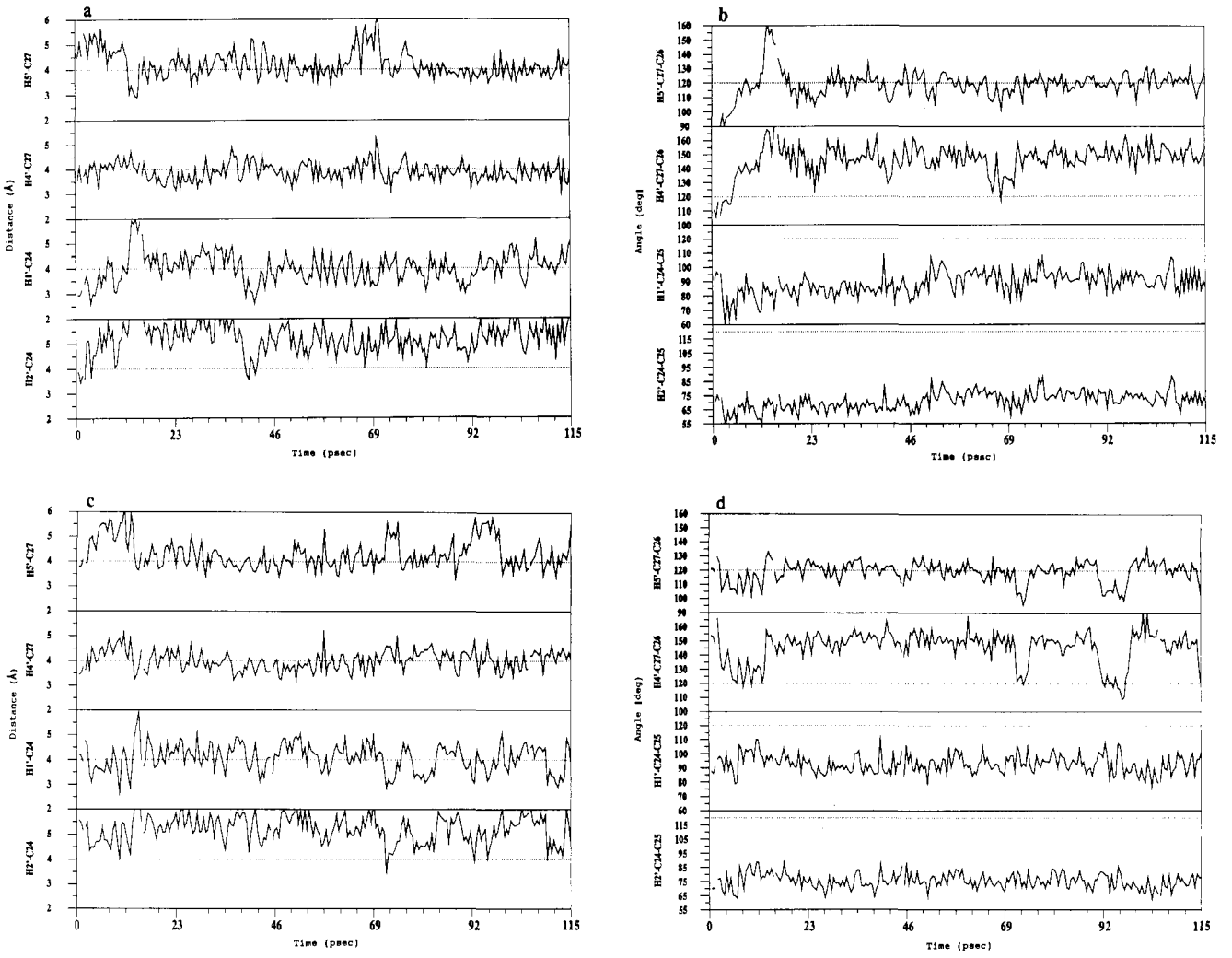

Figure 5. (a and c) The distance (Å) fluctuation over time (ps) between C24 and C27 of dynemicin N hydroquinone and deschlorodynemicin L, respectively, and H5′ and H4′ of guanine 17 and H1′ and H2′ of thymine 5. (b and d) The angle (deg) fluctuation over time (ps) between Hx′–C27–C26 and Hx′–C24–C25 for dynemicin N hydroquinone and deschlorodynemicin L, respectively, where Hx′ = H5′ or H4′ of guanine 17 or H1′ or H2′ of thymine 5.

Therefore, the criteria used in selecting the most likely DNA-hydrogen candidate for abstraction is based on distance and angle. The closest DNA-hydrogen atom to C24 or C27 (the dynemicin carbons that carry the radicals in the transition state) is a candidate if it is near or on the vector extending away from C24 or C27 through C24H or C27H (C25–C24–DNAH or C26–C27–DNAH angle of 120°); if two DNA-hydrogen atoms are nearly equal in distance from C24 or C27, then the one that is the closest to the 120° bond angle is selected.

Calculations

All of the modeling studies were conducted with Polygen's[19] QUANTA/CHARMM software (version 2.1) running on a Silicon Graphics Iris 4D70GT computer. The oligonucleotide and the drug were treated as electrically neutral systems with screened phosphate and carboxylate charges of −0.32 according to Manning counterion condensation theory,[20] and a distance-dependent dielectric was used to approximate screening due to solvent. Switching functions were used in both the energy minimization (EM) and molecular dynamics (MD) for the nonbonded, van der Waals, and electrostatic interactions between 9.5–10.5 Å with an 11.50-Å cutoff.[21] The Verlet algorithm[22] was used to calculate the classical equations of motion for the atoms, and the X–H bonds were fixed by using the SHAKE algorithm[23] during MD.

All EM studies were minimized to a RMS gradient force of ≤0.100 with a conjugate gradient minimizer[24] unless otherwise stated.

The following CHARMM detailed dynamics prescription was used throughout this study. In a 1.5-ps heating phase, the temperature was raised to 300 K in steps of 10 K over 0.05-ps blocks. The MD velocities were reassigned after every step based on the Gaussian approximation to the Maxwell–Boltzmann distribution. This was followed by an equilibration phase in which the velocities were allowed to rescale over the next 13.5 ps in steps of 0.25 ps to stabilize the system within a 300 ± 5 K window. The production phase continued for another 100 ps where the velocities were allowed to rescale every 0.5 ps to keep the system within a 300 ± 10 K window.

A double-stranded B-DNA 10mer with the sequence d-(CTACT_ACTGG)-d(CCAGT_AGTAG), which contains the strongest cut site at G17 (G*, Figure 2), was constructed by using the polymer build function in QUANTA. The crystal coordinates for the intercalated 5′-dCG dinucleotide from the dCG–proflavine complex were obtained from Dr. Helen Berman.[25] The 5′-C_G dinucleotide intercalation cleft was mutated into a 5′-T_A dinucleotide intercalation cleft and graphed into the center TA region of the above 10mer.

The enantiomers of dynemicin N were constructed in CHEMNOTE and transformed into dynemicin A and intermediates along the aromatization pathway in the 3-d construction section of QUANTA. The type of nitrogen (sp^2 or sp^3) used in the various analogues was based on chemical reactivity and the number of electron donating/withdrawing groups that are in conjugation with the nitrogen. Since the dynemicin A nitrogen was not acetylated[1b] under the conditions (acetic anhydride–pyridine, 25

(19) Polygen Corporation, 200 Fifth Avenue, Waltham, MA 02254.
(20) Manning, G. S. *Quart. Rev. Biophys.* **1978**, *11*, 179.
(21) (a) Nilsson, L.; Karplus, M. *J. Comput. Chem.* **1986**, *7*, 591. (b) Tidor, B.; Irikura, K. K.; Brooks, B. R.; Karplus, M. *J. Biomol. Struct. Dyn.* **1983**, *1*, 231.
(22) Verlet, L. *Phys. Rev.* **1967**, *159*, 98.
(23) Ryckaert, J. P.; Cicotti, G.; Berendsen, H. J. C. *J. Comput. Phys.* **1977**, *23*, 327.
(24) Hestenes, M.; Stieffel, E. Report 1659; National Bureau of Standards: Washington, DC, 1952.
(25) (a) Neidle, S.; Pearl, L. H.; Herzyk, P.; Berman, H. M. *Nucleic Acids Res.* **1988**, *16*, 8999. (b) Shieh, H. S.; Berman, H. M.; Dabrow, M.; Neidle, S. *Nucleic Acid Res.* **1980**, *8*, 1, 85.

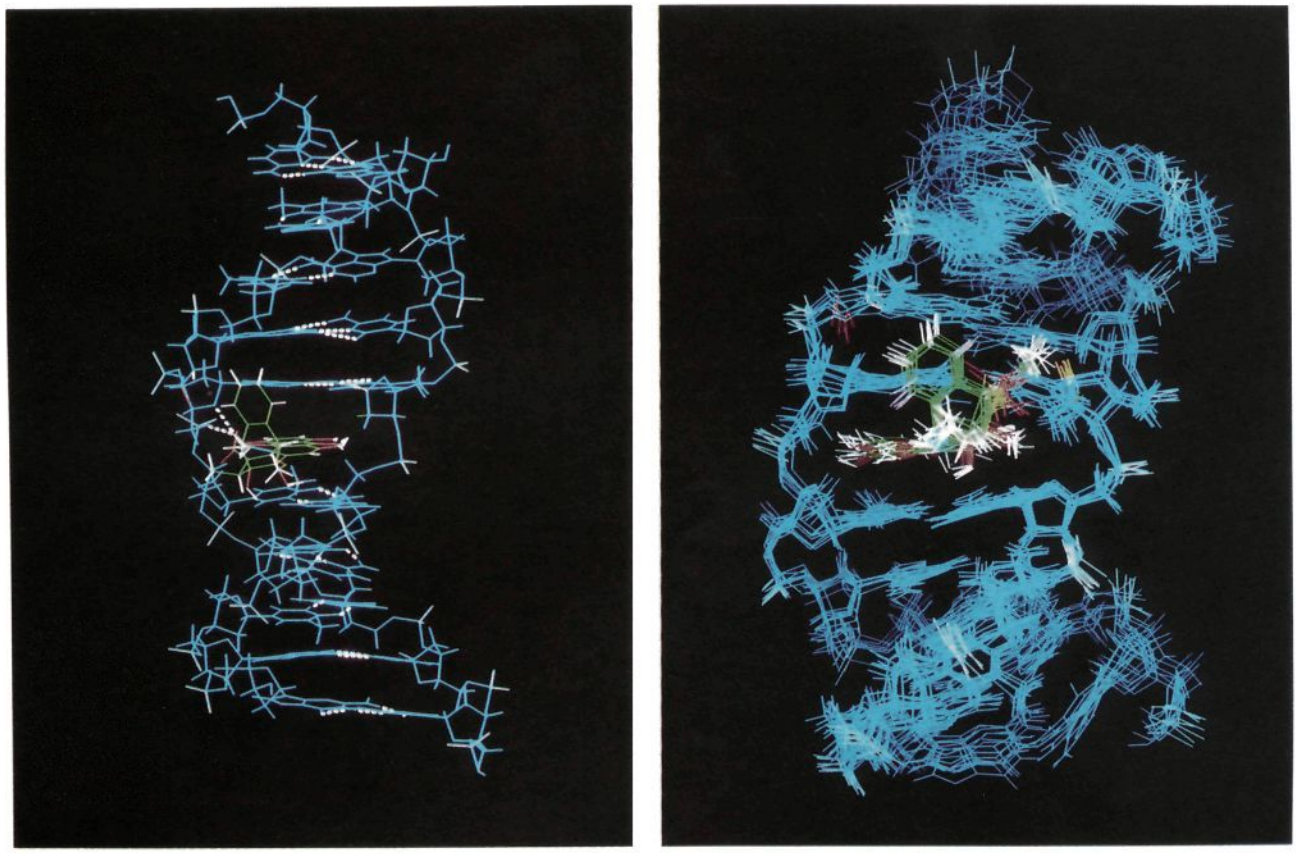

Figure 6. (a, left) The EM intercalation complexes between (2*R*,7*S*)-dynemicin N hydroquinone and d(CTACT_ACTGG)·(CCAGT_AGTAG) oligonucleotide. (b, right) Composite of eight snapshots taken every 5 ps, from 35 to 70 ps, from the dynamics run. The coloring scheme is the same as in Figure 4.

Table II. Statistical Analysis of Histogram Panel B (Figure 2) for Base Preference at the B3 and Ct Site

5′-B3-Py-Pu-Ct domain	B3 base (%)	Ct base (%)
Pu	6/8 (75.0)	7/13 (53.8)
Py	7/13 (53.8)	6/8 (75.0)
A	2/2 (100.0)	1/5 (20.0)
G	4/6 (66.7)	6/8 (75.0)
T	1/5 (20.0)	1/2 (50.0)
C	6/8 (75.0)	5/6 (83.3)

°C) used to make the triacetate and was found to be very nearly planar in the crystal structures, this indicates that the nitrogen in dynemicin A (**1**, Scheme I) and the other quinone-containing analogues (**5** and **7**) are sp^2 in character. In the quinonemethide **3**, the nitrogen is clearly a vinylogous amide and therefore sp^2 in character. In the highly electron-rich hydroquinone analogues (**2**, **4** and **6**) there are three phenols in conjugation with the aniline-like amine; this is expected to make this nitrogen electron-rich and sp^3 in character.

The parameters used for dynemicin were tested by comparing the crystal structures of dynemicin A triacetate[1b] against their EM conformation. Two molecules were found in the asymmetric unit cell. The major difference between the two structures is in the orientations of the freely rotatable acetate, carboxyl, and methoxy appendages and the direction of bowing in the anthraquinone ring system about the D ring (Table III). In molecule 1 (M1) the E ring is bowed down away from the enediyne system by 12° with respect to the C ring, but in molecule 2 (M2) the E ring is bowed up by 17°. Like the MM2//PRDDO calculations of Snyder and Tipsword[8b] our calculations assume planarity for the anthraquinone fragment due to its extended π-system. This assumption seems reasonable since similar anthraquinone ring systems in the daunomycin–[2] and adriamycin–DNA[2d] crystal complexes were planar or very nearly so. The RMS deviation between the two crystal structures and their minimized forms is fairly large (Table III). However, when the acetate, carboxyl, and methoxy appendages along with the D and E rings were removed (–appDE, Table III) from the molecules the RMS deviation dropped significantly. We believe that the reason for

Table III. RMS Deviation between Dynemicin A Triacetate Crystal and Minimized Forms[a]

fragment	M1/M2	M1/M1 min	M2/M2 min
full	0.952	0.463	0.575
–app	0.495	0.292	0.370
–appE	0.249	0.236	0.324
–appDE	0.165	0.200	0.277
–appCDE	0.172	0.175	0.248

[a] M1 and M2 are molecule 1 and 2 from the crystal unit cell, M1min and M2min are the minimized forms of M1 and M2: full (complete molecule comparison), –app (molecule minus the carboxyl, methoxy, and acetate appendages), –appE (minus appendages and E ring), –appDE (minus appendages and D and E rings) and –appCDE (minus appendages and C, D, and E rings).

the large RMS deviation between the two molecules in the crystal unit cell and their minimized form is due mainly to crystal packing forces and to a lesser extent to the assumption that the anthraquinone ring system is planar. The relatively low RMS deviation for the molecules minus the appendages and D and E rings (–appDE) indicates that the CHARMM force field is capable of predicting reasonably well the decalin–enediyne core and its geometric relationship with the anthraquinone ring system.

The different forms of dynemicin were minimized into the nearest local minima. Simulated annealing,[26] which uses MD to explore the conformational space of the molecule, was used to help overcome the local minima problem in locating the lowest energy conformation. The structures with the lowest energy were retained for the dynemicin–DNA docking studies.

The d(CTACT_ACTGG)·d(CCAGT_AGTAG) duplex oligonucleotide containing the 5′-T_A intercalation cleft was minimized in two steps. To correct any error that might have arisen in the backbone interface between the dinucleotide intercalation cleft and the canonical B-form DNA during the grafting, all atoms except the backbone inter-

(26) (a) Kirkpatrick, S.; Gelatt, C. D.; Vecchi, M. P. *Science* **1983**, *220*, 671. (b) Brunger, A. T.; Clore, G. M.; Gronenborn, A. M.; Karplus, M. *Proc. Natl. Acad. Sci. U.S.A.* **1986**, *83*, 3801.

face atoms were fixed, and the oligomer was minimized. The constraints were then removed, and the unrestrained oligomer was minimized with 50 steps of conjugate gradient minimization to locate a local minimum in the vicinity of the starting structure. This final structure was then used in the dynemicin-DNA docking studies.

The different forms of dynemicin were then docked into the intercalation cleft from the minor groove of the DNA with the enediyne pointing in the direction of the strongest cut site. The continuous energy facility in Quanta was used in the docking procedure to find the optimal starting point for EM. The DNA was then constrained and the complex was minimized with 50 steps of conjugate gradient minimization followed by 50 steps of unrestrained minimization prior to molecular dynamics calculation.

The Curves, Dials, and Windows (CDW) analysis package introduced by Ravishanker et al.[27] was used to analyze the MD results in terms of a full set of conformational and helcoidal parameters. The time evolution of the conformational and helcoidal parameters were followed in the analysis, providing a complete description of the dynamical model obtained in the simulation. The structural inferences described below are based on this analysis. A complete CDW graphical description of all the DNA parameters is available from the supplementary material.

The Model

In the dynemicin EM and MD studies only minor conformational changes from dynemicin A occur as one proceeds down the aromatization pathways of Scheme I. Dynemicin A (**1**, Scheme I) contains an sp^2 nitrogen, epoxide, and an extensive hydrogen-bonding network (phenols and nitrogen hydrogens hydrogen bond with the carbonyl oxygens of the quinone) which highly constrains the molecule. The enediyne ring is offset to one end and side of the anthraquinone ring system and leans slightly toward it. In the hydroquinone **2** the amine is sp^3 and freely inverts in the MD to form either a hydrogen bond with the phenol oxygen at C20 or a dipole interaction with the epoxide. The phenols move in concert to maintain a hydrogen-bonding network, pointing toward or away from the enediyne end of the molecule. The tetrahedral amine reduces the ring strain and allows the ends of the enediyne to move, from 3.53 Å for dynemicin A, to 3.41 Å.[28] Rearrangement to the quinonemethide **3** converts the amine back to a sp^2-hybridized vinylogous amide and opens the epoxide. The decalin system relaxes under the reduced ring strain, closing the enediyne end-to-end distance to 3.28 Å. In the diol **4** the bridge head double bond has been removed, the amine is sp^3 in character, and the axial methyl at C4 has moved to a quasi-axial position. This reduces the ring strain considerably, allowing the ends of the enediyne to move within 3.14 Å. The phenols rotate together maintaining a hydrogen-bonding network, and the amine freely inverts but prefers the up position where it participates in the hydrogen-bonding network with the phenols. The alcohol **5** has an anthraquinone ring system and a sp^2 nitrogen. The phenols hydrogen bond with the carbonyl oxygens of the quinone, and the C4 methyl has moved to a quasi-axial position. The sp^2 nitrogen in the B ring constrains the decalin ring system somewhat compared to the diol **4** affording an enediyne end-to-end distance of 3.19 Å and slightly twists the molecule, moving the enediyne away from the anthraquinone ring system. A major conformational change occurs when going from the diol **4** or alcohol **5** to dynemicin N hydroquinone (**6**) or deschlorodynemicin L, respectively. The A ring flips from a quasi-boat to a quasi-chair placing the methyl group in an equatorial position. The quasi-boat to -chair transition twists the aromatic ring away from and to one side of the hydroquinone or quinone ring system giving the (2*S*,7*R*)-enantiomers a right-handed conformation.

In order to determine if the quasi-boat to -chair transition is the primary strain release mechanism for aromatization, as was determined for a simplified esperamicin/calicheamicin core,[9c] distance constraint minimization followed by single point unrestrained energy calculations were carried out on the diol **4** and alcohol **5** A-ring quasi-boat and -chair forms. As the enediyne end-to-end distance approached the predicted aromatization transition-state distance of 2.06 Å,[9b] the lowest energy pathway for the diol **4** switches from the quasi-boat to the -chair form at 2.78 Å (Figure 3a), suggesting that the ring flip occurs before aromatization. However, the lowest energy pathway for the alcohol **5** was via the quasi-boat form, converging after aromatization with the two different forms being roughly equal in energy. The unconstrained minimized diol **4** A-ring quasi-chair form has an end-to-end enediyne distance of 2.96 Å and is calculated to be 2.37 Kcal higher in energy relative to the A-ring quasi-boat conformer. Like the A-ring quasi-boat conformer of the alcohol **5** the A-ring quasi-chair conformer of the diol **4** has a right-handed twist for the (2*S*,7*R*)-enantiomers which is amplified as the ends of the enediyne are pulled together to the aromatic forms. The right-handed twist makes the molecules more complementary to the minor groove of the right-handed B-DNA (Figure 3b).

Different modes of dynemicin-DNA binding (major groove intercalation, groove and backbone binding, and minor groove intercalation) were investigated. The docking of dynemicin as a major groove intercalator was found to be inconsistent with the experimental data in that H5′ points into the minor groove, while H5″ points straight out into the bulk solvent and not into the major groove making it highly unlikely that an enediyne bound in the major groove would be able to abstract a C5′-hydrogen. The L-shape nature of dynemicin makes it an unlikely major or minor groove binder since the grooves are straight and narrow and not L-shaped. A backbone/minor groove binding model for the (2*R*,7*S*)-enantiomers was found that placed the enediyne in the minor groove, while the anthraquinone phenols formed hydrogen bonds with the phosphate backbone of both DNA strands. However, this model was ruled out because in the MD it was found to be inconsistent with H5′ or H5″ abstraction. Docking of dynemicin in the DNA as a minor groove intercalator was found to be qualitatively consistent with the experimental data.

The minimized (2*S*,7*R*)-dynemicin enantiomer-DNA complexes gave the lowest minimized energy when the long axis of the anthraquinone ring system was approximately perpendicular to the long axis of the DNA base pairs in the intercalation cleft (Figure 4a). This is similar to the intercalation mode found for the anthracyclines daunomycin[2] and adriamycin.[2d] The (2*R*,7*S*)-enantiomer-DNA complexes gave the lowest minimized energy when the long axis of the anthraquinone is approximately parallel to the base (Figure 5a), which is in line with the intercalators terpyridine platinum,[29] ellipticine,[30] tetramethyl-*N*-methylphenanthrolinium,[30] and the acridines.[25b,31] The EM complexes for both enantiomers of dynemicin N hydroquinone and deschlorodynemicin L predict a 4′-hydrogen abstraction from one strand and a 1′-hydrogen abstraction from the other (Figures 4a and 6a) and not the experimentally observed 5′-hydrogen abstraction. This is not an uncommon problem since a minimizer moves you deeper into the potential well closest to the starting point. Since the intercalation cleft conformation is from the dCG-proflavine crystal structure (a parallel intercalater), it is possible that our starting point is less than ideal when used to model a perpendicular intercalater. One way to overcome the local minima problem, at least in part, is to allow MD to find the thermodynamically most stable family of conformations for the guest-host complex.[26]

In the MD studies only the (2*S*,7*R*)-dynemicin N hydroquinone-DNA complex underwent the conformational changes needed for the model to comply with the observed experimental

(27) Ravishanker, G.; Swaminathan, S.; Beveridge, D. L.; Lavery, R.; Sklenar, H. *J. Biomol. Struct. Dyn.* **1989**, *6*, 4, 669.

(28) It has been shown that the ground-state enediyne end-to-end distance is useful in predicting if an enediyne system will aromatize at ambient temperatures (ref 9a). It should be noted that exceptions exist (ref 9c). By using the computationally more intense MM2//PRDDO method, it has been shown that the strain energy developed in the transition state is a better predictor (ref 9b-d).

(29) Wang, A. W.-J.; Nathans, J.; van der Marel, G.; van Boom, J. H.; Rich, A. *Nature* **1978**, *276*, 471.

(30) Jain, S. C.; Bhandary, K. K.; Sobell, H. M. *J. Mol. Biol.* **1979**, *135*, 813.

(31) (a) Sokore, T. D.; Reddy, B. S.; Sobell, H. M. *J. Mol. Biol.* **1979**, *135*, 763. (b) Reddy, B. S.; Seshadri, T. P.; Sakore, T. D.; Sobell, H. M. *J. Mol. Biol.* **1979**, *135*, 787.

results.[32] On the basis of PRDDO calculations,[9b] this is not unreasonable since the diradical intermediate is more benzene-like then enediyne-like. Therefore, the model of the dynemicin N hydroquinone–DNA complex should more accurately predict which DNA backbone hydrogen(s) are abstracted. The conformational changes in the complex are driven by hydrogen bonding and electrostatic and van der Waals interactions. Within the first 3 ps the secondary amine in dynemicin N begins inverting to hydrogen bond with both N3 of adenine 6 and O2 of thymine 5, and the phenols OH15, OH13, and OH11 turned toward the enediyne end of the dynemicin. This orientation maintained the intrahydrogen-bonding network and allowed OH11 to hydrogen bond with O4′ and O5′ of adenine 16 and OH13 to hydrogen bond with N7 of adenine 16. Over the next 16 ps the phenols OH18 and OH20 turned toward the enediyne end of the molecule forming a hydrogen bond between OH20 and O2 of thymine 5. Over this same time period the amine stopped inverting and formed a very strong hydrogen bond with N3 of adenine 6. Simultaneously the DNA backbone dihedral angles for the center 5′-CT_AC/GT_AG base pairs underwent transitional changes. These changes increased the helix twist of the 5′-T_A/T_A step from 17° to ~23° and simultaneously produced an increased tilt and roll in the 5′-CT/AG and 5′-AC/GT steps and a decrease in the tilt and roll in the 5′-T_A/T_A step which exposed the H5′ of guanine 17 to C27 of dynemicin (Figure 4b). Over the next 33 ps the helicoidal parameters continued to slide producing a stable bent intercalated B-form DNA. The helix twist of the intercalation cleft and base pair rise stabilized around average values of 28° (unwinding angle of 8°) and 6.4 Å. During this time dynemicin settled into the intercalation cleft forming hydrogen bonds periodically between NH1, OH18, O18, OH20, OH11, OH13, and OH3 of dynemicin with N3, N7, NH6 of adenine 6, O2 of thymine 5, O5′ and O4′ of adenine 16, N7 and O2P of adenine 16, and O4′ of cytosine 7, respectively (Figure 4 (parts b and c)). The hydrogen bonds anchor the drug in the intercalation cleft in a way that positions H5′ of guanine 17 near C27 (Figure 5a) and in line with the C27–C27H bond (radical orbital) of dynemicin (Figure 5b). Dynemicin C24 is near H1′ and H2′ of thymine 5 on the opposite strand. Throughout the remaining 69 ps the system remained stable (Figure 4d) with only minor fluctuations in the backbone and helicoidal parameters. The terminal base pairs of the oligomer also stabilized over the MD calculation; however, the amplitude in the backbone and helicoidal fluctuation was expectedly higher due to end effects.

The (2*R*,7*S*)-dynemicin N hydroquinone–DNA complex quickly stabilized in the MD. However, the left-handed twist of this enantiomer orientates C24 and C27, so that they point up and down the minor groove (Figure 6b) and not toward the DNA backbone making direct DNA hydrogen abstraction by radicals at either of these positions unlikely.

Deschlorodynemicin L (**7**) failed to produce a dynamically stable model that was consistent with experimentally observed C5′-hydrogen abstraction from guanine 17 when the proflavine intercalation cleft geometry was used as the starting point in the calculation. Within the first 4 ps the deschlorodynemicin L–DNA complex underwent the needed conformational changes to place H5′ of guanine 17 near C27 and in line with the C27–C27H bond of dynemicin. However, the Watson and Crick hydrogen bonds between adenine 16 and thymine 5 were disrupted, and thymine 5 rolled slightly out of its reading frame. By 8 ps the drug had slightly turned and moved partially out of the intercalation cleft, pointing C27 away from the DNA backbone and into the solvent environment and C24 toward H1′ of thymine 5. Over the same time period, the DNA reverted into the conformation space near the starting point. This slight change in the position of the drug produced several hydrogen bonds between the drug and the intercalation cleft and reduced a repulsive dipole–dipole interaction between the quinone carbonyl at C20 and O2 of thymine 5. Due to the difference in the electrostatic interactions within the deschlorodynemicin L– and dynemicin N hydroquinone–DNA complexes, the deschlorodynemicin L–DNA complex was unable to undergo the conformational changes needed to reach a dynamically stable complex that predicted H5′ of guanine 17 to be abstracted. However, when the dynamically equilibrated DNA from the 100-ps step of the dynemicin N hydroquinone–DNA calculation was used as the DNA starting point for the deschlorodynemicin L–DNA complex and subjected to the EM MD protocol, a dynamically stable model resulted with little to no changes in the DNA conformational parameters. By the end of the heat and equilibration phases of the MD, the drug had settled into the intercalation cleft, planting C27 near (Figure 5c) and in line with H5′ of guanine 17 (Figure 5d). Like dynemicin N hydroquinone, deschlorodynemicin L reads the base pairs making up the intercalation cleft by forming hydrogen bonds periodically between N1, OH18, O18, OH3, OH11, O15, and OH15 of deschlorodynemicin L with N3, N7, NH6 of adenine 6, N3 of adenine 6, O2 and O4′ of cytosine, and O2 of thymine 15, (O4′, O5′, and N7 of adenine 16, NH6 of adenine 16, and O4 of thymine 15, respectively. The helix twist and base pair rise remained stable, fluctuating with average values of 28° and 6.4 Å, respectively.

Discussion

It is believed that dynemicin A exerts its biological effect by causing DNA strand breaks. Presumably, in the two-electron-reducing environment of the NADPH–dynemicin DNA system,[7] dynemicin A must be first reductively activated to the hydroquinone prior to intercalation, which then rearranges to the quinonemethide followed by nucleophilic attack and/or protonation producing the diol and/or alcohol. Due to the relaxed ring strain the diol–DNA and/or alcohol–DNA complex can now undergo conformation changes leading to diradical generation and DNA cleavage, via a Bergman type reaction and DNA hydrogen abstraction.

The actual dynemicin intermediate that intercalates into the DNA and leads to DNA strand breaks is unclear. In the total synthesis of 7-*con*-*O*-methylnogarol, Hauser's group[33] has shown that reductive opening of the C9–C10 epoxide was very slow with two-electron-reducing agents and that the addition of base substantially enhanced the rate of epoxide opening. The work of Koch's group on the reduction of anthracyclines has shown that the quinonemethide has a half-life of 53 s, 63 s, and longer for daunomycin,[12b] adriamycin,[12c] and menogaril,[12d] respectively. The calculated energy difference for dynemicin diol of 2.36 kcal between the quasi-boat and -chair forms gave a K_{eq} of 0.996 in favor of the quasi-boat form at 37 °C. The above findings together with the calculations by Snyder and Tipsword[8b] suggest that all of the molecules depicted in Scheme I have a finite half-life once dynemicin A is reduced and could intercalate into DNA, and what determines which one binds depends on how far away from the DNA the reduction step takes place. However, it is certain that the diol **4** or alcohol **5** must be intercalated prior to aromatization for DNA cleavage to occur.[7]

Like dynemicin N hydroquinone (**6**) and deschlorodynemicin L (**7**) the epoxide hydroquinone **2** and quinonemethide **3** phenols form hydrogen bonds and electrostatic interactions with the intercalation cleft. A hydrogen bond between OH18, NH1, and/or O20 with either N7 or N3 of adenine 6 or O2 of thymine 5 could facilitate the rearrangement to the quinonemethide **3**, or one of its resonant forms, and the opening of the epoxide by deprotonating the epoxide hydroquinone **2**. The resulting bifurcated proton could activate the quinone methide to nucleophilic attack. The position of the quinonemethide **3** in the intercalation cleft places C8 up off of the floor and in about the center of the minor groove of the DNA which makes it highly accessible and directionally correct for nucleophilic attack by bulk water. On the other hand, the hydrogen bonds observed between the OH11 and OH13 of the quinonemethide **3** and the DNA backbone could assist in the

(32) Molecular dynamics on the A-ring quasi-chair (2*S*,7*R*)-diol enantiomer–DNA complex, in which the enediyne end-to-end distance was constrained to 2.06 Å, produced a model that was consistent with experimental results, whereas the constrained quasi-boat form did not.

(33) Hauser, F. M., personal communication.

rearrangement to the alcohol **5**; this rearrangement has been calculated[8b] to be exothermic by 22.8 Kcal. In the (2*S*,7*R*)-dynemicin A conformer, the enediyne is offset to the right side and front end of the anthraquinone ring system when viewed from the enediyne end of the molecule, with the enediyne pointing up. As the diol **4** and alcohol **5** are converted to dynemicin N hydroquinone (**6**) and deschlorodynemicin L (**7**) they develop a right-handed twist and become more complimentary with the right-handed B-DNA. These results suggest that the DNA may be acting as a self-immolative catalyst by way of deprotonation and/or reprotonation and as a chiral catalyst[34] leading to the diradical transition state and DNA hydrogen abstraction.

In this modeling study only the minor groove intercalated (2*S*,7*R*)-dynemicin N hydroquinone and deschlorodynemicin L enantiomers produced a dynamically stable model that is consistent with the affinity cleavage results. Furthermore, the (2*S*,7*R*)-enantiomers intercalate in the DNA with the long axis of dynemicin perpendicular to the intercalation cleft base pairs, and the helix twist and base pair rise of the MD-equilibrated complexes are consistent with the intercalation mode, helix twist, and base pair rise found in the daunomycin–[2] and adriamycin–DNA[2d] crystal complexes. These results strongly predict that the (2*S*,7*R*)-enantiomer is the correct absolute stereochemical form of dynemicin.

The fact that the deschlorodynemicin L–DNA was unable to undergo the transitions needed to produce a model that is consistent with the experimental results is believed to be due to the hydrogen-bonding potential used in CHARMM for the DNA Watson and Crick hydrogen bonds.[21] In the first few steps of the MD, the complex started the transition placing H5′ of guanine 17 near C27 of deschlorodynemicin L. However, this caused thymine 5 to roll out of its reading frame, and the Watson and Crick hydrogen bonds were broken. In the next few steps the DNA hydrogen-bonding potential pulled the thymine back into its reading frame and forced the drug out. Presumably, the system would have reached an equilibrium state in due course if the DNA hydrogen-bonding potential had not stepped in. It is interesting that deschlorodynemicin L did form a dynamically stable complex with the MD-equilibrated DNA from the dynemicin N hydroquinone–DNA complex that is in agreement with the cleavage affinity results. This demonstrates the power as well as limitations of MD and serves as an internal validation of the calculation.

The findings of the affinity cleavage[7] study together with this modeling study suggest that dynemicin A does not cause the DNA double strand breaks that are staggered by three base pairs in the 3′-direction concomitantly but instead produces a single strand break at the base to the immediate 3′-side of the intercalation cleft via an H5′ abstraction by the carbon-centered radical at C27. The fate of the radical at C24 is less clear; the closest and most in line DNA hydrogen is H1′ of thymine 5. Abstraction of H1′ has been shown to cause abasic sites;[35] however, under the conditions of the affinity cleavage experiments (nonbasic) this is not expected to produce DNA strand breaks. The next most likely candidate for abstraction by a C24-centered radical is H2′. An H2′ abstraction has not previously been reported but is not expected to produce DNA breaks.

Dynemicin exhibits a sequence specificity for cleaving DNA of 5′-B2-B1-Ct in which the B2-B1 site make up the intercalation cleft. The drug preference for the B2-B1 site is 5′-Py-Pu ≫ Py-Py > Pu-Py > Pu-Pu. For example, 83.3% of 5′-TA and 71% of 5′-TG sites resulted in strong cuts, with little or no regard for the type of bases at positions B3 or Ct. Furthermore, 80.0% of the 5′-Py-Pu and 100% of 5′-TA cut sites have a strong or medium cleavage site on the opposite strand staggered by three base pair in the 3′-direction. These staggered cut sites can be explained by considering the symmetry of the 5′-Py-Pu-Ct/3′-Ct-Pu-Py double-stranded dinucleotide and the drugs low specificity for the B3 and Ct bases. If the drug intercalates into the 5′-Py-Pu sequence with the enediyne ring pointing in the 3′-direction (relative to the top strand), then the top strand is cut, and the 5′-Py-Pu-Ct site results. However, if the drug intercalates with the enediyne pointing in the 5′-direction, the bottom strand is cut, and the 3′-Ct-Pu-Py site is produced. The hydrogen-bonding network between the 5′-Py-Pu intercalation cleft and the diol **4** or the alcohol **5** provide the binding energy to anchor the activated drug in the proper reading frame for efficient DNA hydrogen abstraction. Changing the bases in the preferred sequence would either reduce the number of hydrogen bonds (decrease the binding energy) and/or change the reading frame making DNA hydrogen abstraction less efficient.

Conclusions

With the use of in vacuo energy minimization and molecular dynamics techniques a model for the dynemicin–DNA complex has been constructed that is consistent with the affinity cleavage study.[7] The model has been used to predict the absolute stereochemistry of dynemicin A to be the (2*S*,3*S*,4*S*,7*R*,8*R*)-enantiomer, to support the proposed intercalation mode of binding to DNA, to explain the pattern and sequence specificity of cleavage, and to suggest a mechanism in which the DNA may be acting as a catalyst in the aromatization of the intercalated dynemicin leading to its own destruction.

Acknowledgment. We are grateful to Drs. Y. Sugiura, J. Clardy, and G. D. VanDuyne for providing us with their results prior to publication. We also thank Drs. S. Swaminathan and G. Ravishanker for many useful discussions on molecular dynamics and analysis of the results. This work was supported by grants to D.L.B. from the National Institutes of Health (GM-37909) and from the Bristol-Myers Squibb Company via a Connecticut Cooperative High Technology Research and Development Grant.

Supplementary Material Available: Complete Curves, Dials, and Windows[27] graphical analysis of all the DNA parameters over the time course of the molecular dynamics simulation (12 pages). Ordering information is given on any current masthead page.

(34) Lerner, R. A.; Benkovic, S. J. *BioEssays* **1988**, *9*, 107.
(35) Kappen, L. S.; Chen, C.; Goldberg, I. H. *Biochemistry* **1988**, *27*, 4331.